Proceedings of the International Symposium on Acoustic Tomography and Thermometry
Tokyo, Japan, 8-9 February, 1999 (Hosted by JAMSTEC)

The Acoustic Thermometry of Ocean Climate (ATOC) Project: Towards depth-averaged temperature maps of the North Pacific Ocean

Brian D. Dushaw and the ATOC Group* (Applied Physics Laboratory, College of Ocean and Fisheries Sciences, University of Washington, Seattle, WA 98105)
e-mail: dushaw@apl.washington.edu

ABSTRACT

The ATOC Project has aquired trans-Pacific acoustic data from two acoustic sources: one located on Pioneer Seamount off the coast of California, the other located north of Kauai, Hawaii. Transmissions from these sources are detected by U.S. Navy SOSUS arrays located throughout the North Pacific. The time series of acoustic travel times from the Pioneer Seamount and Kauai transmissions are about 1 1/2 and 1 year long, respectively. Both time series have highly irregular sampling because of marine mammal protocols and temporary cable failures; the timeseries derived from the two acoustic sources overlap by about 75 days. These acoustic data are used to accurately estimate ocean temperature. The overlapping time series for the first time allow estimates of temperature maps of the North Pacific basin using long-range acoustics because the acoustic paths from these sources criss-cross the North Pacific. Maps of depth-averaged temperature of the North Pacific Ocean are derived using the time series collected through 1998.

INTRODUCTION

The Acoustic Thermometry of Ocean Climate (ATOC) program has achieved its original goal of acquiring time series of acoustic travel time over basin-scale paths (Figure 1) and using that data to accurately determine range- and depth-averaged ocean temperature [1-3]. Acoustic sources were deployed on Pioneer Seamount near San Francisco in October 1995 and on the north slope of the Hawaiian island of Kauai in July 1997. The Pioneer Seamount and Kauai sites were selected to allow much of the acoustic energy to leave the source without interaction with the ocean bottom. To date several time series of acoustic data of about 15 months duration have been obtained from acoustic transmissions from the Pioneer Seamount acoustic source to receiving arrays located throughout the North Pacific ocean, including two moored vertical line arrays of hydrophones (VLAs) and U.S. Navy SOund SUrveilance System (SOSUS) bottom-mounted horizontal line arrays. The data have been collected since about 1 January 1996. The travel time data are obtained in near real time, and estimates of range-averaged temperature are obtained within a few days after the data are collected.

---

* The Acoustic Thermometry of Ocean Climate (ATOC) Group is: A.B. Baggeroer, D. Menememlis [now at JPL], and C. Wunsch (MIT); T.G. Birdsall, K. Metzger (U. Mich.); C. Clark (Cornell U.); J.A. Colosi (WHOI); B.D. Cornuelle, M. Dzieciuch, W. Munk, P.F. Worcester (SIO); D. Costa (U. Calif., Santa Cruz); B.D. Dushaw, B.M. Howe, J.A. Mercer, R.C. Spindel (APL-U. Wash.); A.M.G. Forbes (CSIRO, Hobart).

A detailed analysis of the acoustic data obtained at up to 5 Mm range and its inversion for ocean temperature has been described by Dushaw et al. (2) and Dushaw (3). Range- and depth-averaged temperature along the acoustic paths can be estimated to high accuracy by acoustic thermometry, and those average estimates are robust to modeling assumptions. This brief paper describes the inversion of acoustic data obtained from both the Pioneer and Kauai acoustic sources for three-dimensional maps of the North Pacific Ocean. Since little resolution of variability with depth is available (2), maps of sound speed averaged over 0–1000 m depths are derived.

TRAVEL TIME VARIABILITY

The suitability of the acoustic data for acoustic thermometry has been previously described. The data used for inversion are the time series of ray arrivals extracted from the acoustic receptions. Figures 2 and 3 show time series of ray travel times derived from Pioneer and Kauai acoustic transmissions. The mean of the travel times has been removed to better show the oceanic thermal variability. In all cases, the various timeseries in each panel can be identified with a particular acoustic ray predicted using the Levitus ocean atlas (4,5). Typically 5–8 ray arrivals are found on each acoustic path. Note that the data obtained from the Kauai source transmissions shows much greater "high" frequency (< 100 day timescales) variability than the Pioneer source transmissions. Apparently the region around Hawaii has greater mesoscale variability. This phenomena was previously reported by Spiesberger and Metzger (6). The acoustic ray paths generally turn below 100–200 m depths near Hawaii (Figure 5), so the observed variability is probably caused by displacement of the main thermocline; the variability is clearly not in the near-surface. Travel times to receivers **k** and **l** show a strong annual cycle (not shown); rays to these receivers are mainly surface reflecting the entire length of the 5 Mm long paths.

MODEL FOR SOUND SPEED VARIABILITY USED FOR INVERSION

The variation in the ray travel times, ΔT, is given by

$$\Delta T_i = -\int_{\Gamma_i} \frac{\delta c(\mathbf{x}, t)}{c_0^2(\mathbf{x})}\, ds$$

For the purposes of this mapping excercise here, the value of δc is modeled as

$$\delta c(x, y, z) = \sum_{i=1}^{n_z} \eta_i(z) \left[A_{00}^{0i} + \sum_{j=1}^{n} \begin{pmatrix} A_{0j}^{1i} \cos(k_j x) + \\ A_{0j}^{2i} \sin(k_j x) + \\ A_{0j}^{3i} \cos(k_j y) + \\ A_{0j}^{4i} \sin(k_j y) \end{pmatrix} + \sum_{j,l=1}^{n_x, n_y} \begin{pmatrix} A_{jl}^{5i} \cos(k_j x) \cos(k_l y) + \\ A_{jl}^{6i} \cos(k_j x) \sin(k_l y) + \\ A_{jl}^{7i} \sin(k_j x) \cos(k_l y) + \\ A_{jl}^{8i} \sin(k_j x) \sin(k_l y) \end{pmatrix} \right]$$

where $\eta_i(z)$ are a set of vertical modes (3), and $k_n = 2\pi n/L, n = 1, 2, 3\ldots$. L is a domain size greater than the region of interest. Zero wavenumbers are obviously included. The A's are the model parameters to solve for. The number of parameters can be calculated with the formula,

$$N_{parameters} = N_V\,(1 + 4\,(\,N_H + 1\,)\,N_H)$$

where N_V and N_H are the number of vertical modes and number of wavenumbers respectively. If an inversion uses 5 modes in the vertical and 20 wavenumbers there are a total of 8405 parameters, A^q_{jl}, to solve for.

With this model, the equation for travel times may be written, $\mathbf{d} = \mathbf{GA} + \mathbf{n}$ where $\mathbf{d}$ is a vector of ray travel times, $\mathbf{G}$ is the matrix whose components consist of the integral of one of three dimensional functions for sound speed over an acoustic ray path, $\mathbf{A}$ is the vector of model parmeters to solve for, and $\mathbf{n}$ is noise. As described in detail by Dushaw, et al. (2), typical values for noise in the travel times are 1200–2500 ms^2. In this case, the noise is mainly caused by complications to the receptions resulting from near-source and near-receiver bottom interaction (2).

A major component of the inversion of the travel times is the relative weights to be assigned to the model parameters through $\mathbf{R_{AA}}$. From an assumed correlation function

$$C(x) = <x^2>\exp(-|x|/(L'/2pi)) = <x^2>\exp(-k_0|x|)$$

the spectrum, or weighting, of wavenumbers in two dimensions (k_x, k_y)is

$$S(k) = \frac{2<x^2>}{L'}\,\frac{1}{(\,k_x^2 + k_y^2 + k_0^2\,)^{3/2}}$$

where $k_0 = 2\pi/L'$ gives an e-folding length scale, L'. k_0 also prevents the variance from going to infinity at zero wavenumber. The prime on L' is to separate it from L in the discrete wavenumbers used in the ocean model, $2\pi n/L$, for which $L = 7000$ km.

INVERSION

With $\mathbf{G}$ and the travel times, $\Delta\mathbf{T}$, the inverse gives the model parameters $\mathbf{A}$. One requires an a priori model covariance matrix, $(\mathbf{R_{AA}})_{jj} = <(A_j)^2>$ (assumed diagonal), and an a priori data noise covariance matrix $(\mathbf{R_{nn}})_{ii} = <(n_i)^2>$ (also assumed diagonal). In general, $n_i \neq n_j$ for $i \neq j$. Then if $\mathbf{R_{dd}} = \mathbf{G}\,\mathbf{R_{AA}}\,\mathbf{G^T} + \mathbf{R_{nn}}$, the inverse operator particular to the choice of ocean model and a priori variances is $\mathbf{L} = \mathbf{R_{AA}}\,\mathbf{G^T}\,\mathbf{R_{dd}^{-1}}$. The model solution is $\hat{\mathbf{A}} = \mathbf{L}\,\mathbf{d}$. The model error covariance matrix is $\mathbf{E} = \mathbf{R_{AA}} - \mathbf{L}\,\mathbf{G}\,\mathbf{R_{AA}}\,(\mathbf{L}\,\mathbf{G})^\mathbf{T}$. In general, the model solution and error covariance are transformed into the physical space which is of greater interest to oceanographers. In the present case we apply an operator, $\mathbf{O}(x, y)$ that results in a two-dimensional map of sound speed

averaged over 0–1000 m depths. The map of sound speed is just $M(x, y) = \mathbf{O}\,\mathbf{A}$, while the corresponding uncertainty map is given by the diagonal of $\mathbf{O}\,\mathbf{E}\,\mathbf{O}^{\mathbf{T}}$. In the case of acoustic tomography, much of the information about the line-integral sound speed estimates is carried in the off-diagonal elements of this error covariance, however. While the two-dimensional error maps may have large uncertainty at any one point, the uncertainty of an average along an acoustic path is quite small.

SOME MAPS

Figures 5 and 6 show two sample objective maps of the North Pacific Ocean using the ATOC data. These are maps of 0–1000-m depth-averaged sound speed, with values ranging from -0.5 m/s (dark blue) to +0.5 m/s (dark red). The uncertainty map is superimposed using the white contour lines. The yearday associated with each map is indicated by the bottom panel. The travel time residuals associated these objective maps are presently too large by far, but this is the first attempt at constructing these maps. Further, because most of the receiver positions are classified, fictive positions are used for the inversion, and so the fit cannot be expected to be as good as when the true positions are used. [Objective maps with the true positions will be completed soon.] The horizontal correlation length assumed for the inversion is shown by the width of the uncertainty contour lines across an acoustic path. Since the ray paths do not sample to the ocean surface in the region near Hawaii like they do in the northern or eastern pacific, the maps shown here must be interpreted carefully. To best estimate the ocean state, the acoustic data might be better employed by combining them with other data using a dynamical ocean model and data assimilation, but it is still important to make the zero-order ocean estimate for a variety of obvious reasons, e.g. a sanity check.

CONCLUSIONS

The work described here is at the level of a mapping excercise at the moment. This work will continue with the goals of making the most statistically consistent maps possible, and then comparing and combining these maps with other data such as the Hawaiian Ocean Timeseries (HOT) or TOPEX/POSEIDON altimetric data. Even with the brief timeseries that are available, one catches a glimpse of the impressive possiblities of the acoustic data. One can imagine what a complete 3-year timeseries of maps of the North Pacific would look like, and what an interesting oceanographic observation this would be. We hope that the results described here are just the beginning of a long and continuous timeseries.

REFERENCES

[1] The ATOC Consortium, "Observing ocean climate change: Comparison of acoustic tomography and satellite altimetry with circulation modeling," *Science*, vol. 281, pp. 1327–1332, 1998.

[2] B. D. Dushaw, B. M. Howe, J. A. Mercer, R. C. Spindel, and the ATOC Group, "Multimegameter range acoustic data obtained by bottom-mounted hydrophone arrays for measurement of ocean temperature," *IEEE J. Ocean. Engin.*, in press, April 1999.

[3] Dushaw, B. D., "Inversion of multimegameter range acoustic data for ocean temperature," *J. Ocean. Engin.*, in press, April 1999.

[4] S. Levitus, R. Burgett, and T. P. Boyer, *World Ocean Atlas 1994, Vol. 3: Salinity*. NOAA Atlas NESDIS 3, Washington, DC: U.S. Government Printing Office, 1994.

[5] S. Levitus and T. P. Boyer, *World Ocean Atlas 1994, Vol. 4: Temperature*. NOAA Atlas NESDIS 4, Washington, DC: U.S. Government Printing Office, 1994.

[6] Spiesberger, J. L., and K. Metzger, "Listening for climatic temperature change in the northeast Pacific: 1983–1989," *J. Acoust. Soc. Am.*, vol. 92, pp. 384–396, 1992.

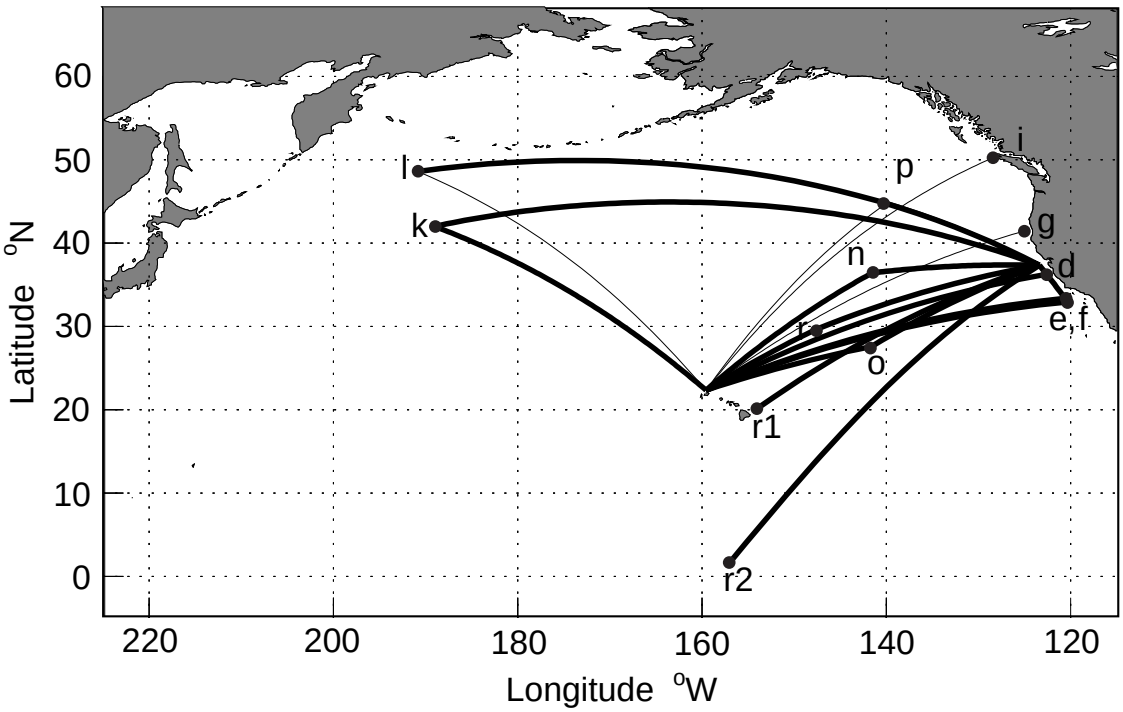

Figure 1. The ATOC array. The array spans most of the North Pacific Ocean. Acoustic paths to the various receivers from the Kauai and Pioneer Seamount acoustic sources are shown. Paths noted by heavy lines are those for which ray travel time data have been derived. Paths noted by light lines have weaker or noisier receptions in which clear ray arrivals are not evident, but travel time data may eventually be derived for these paths. Modified from (2).

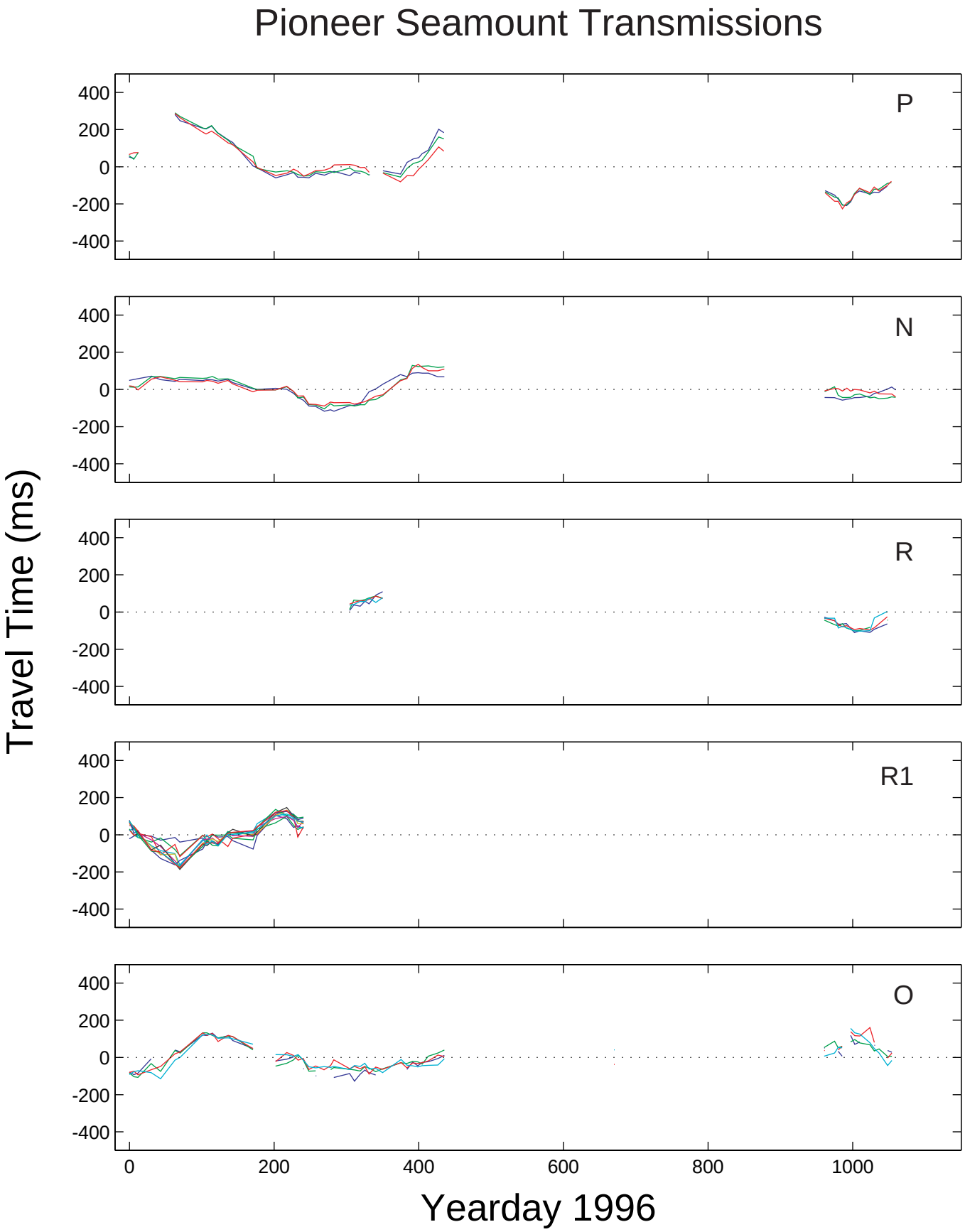

Figure 2. Travel time variability observed on the acoustic paths from Pioneer Seamount to various receivers as indicated. Modified from (2).

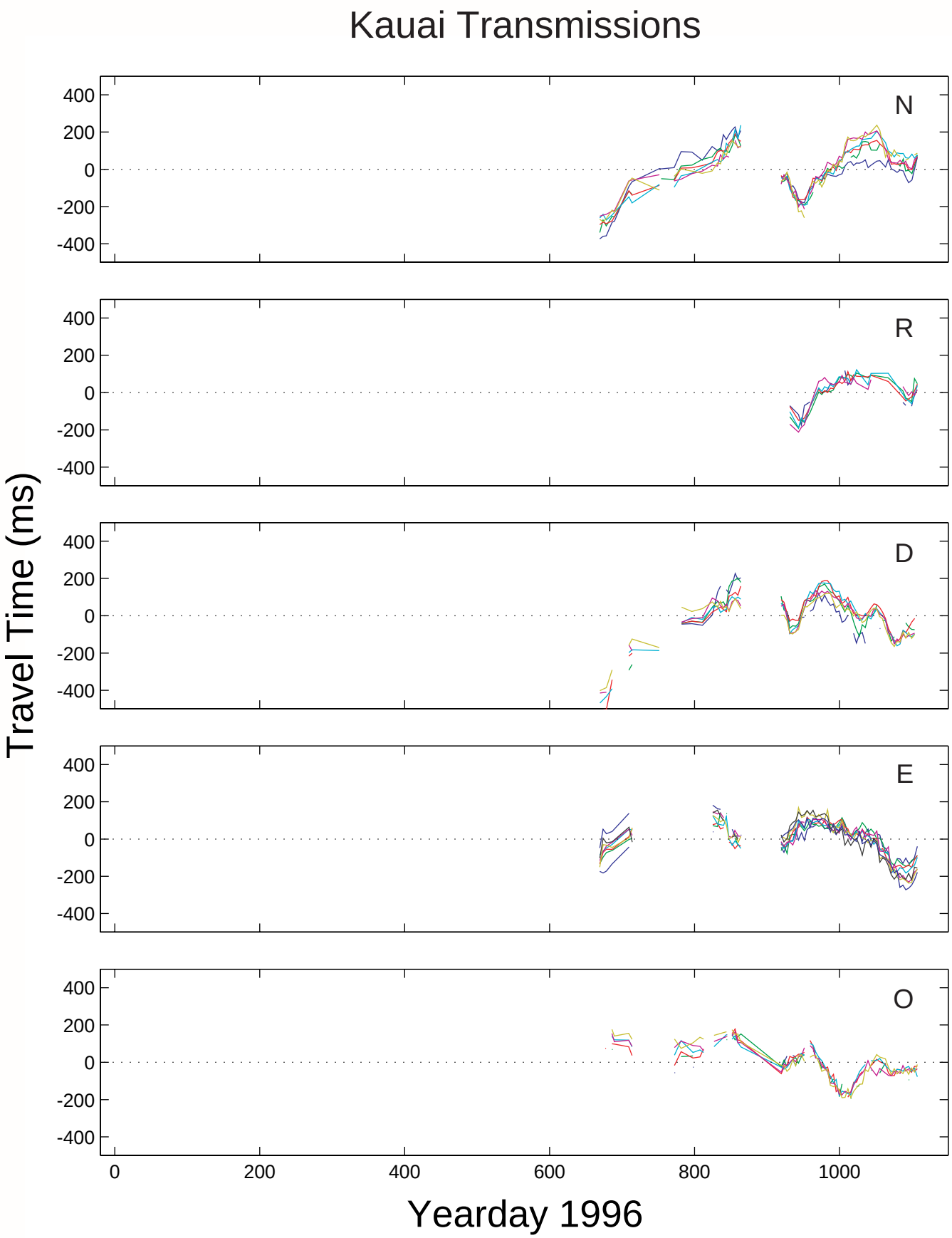

Figure 3. Travel time variability observed on the acoustic paths from Kauai to various receivers as indicated. The data shown in Figure 2 and here are both for the region between California and Hawaii, yet the travel times from the Kauai acoustic source show much greater mesoscale variability.

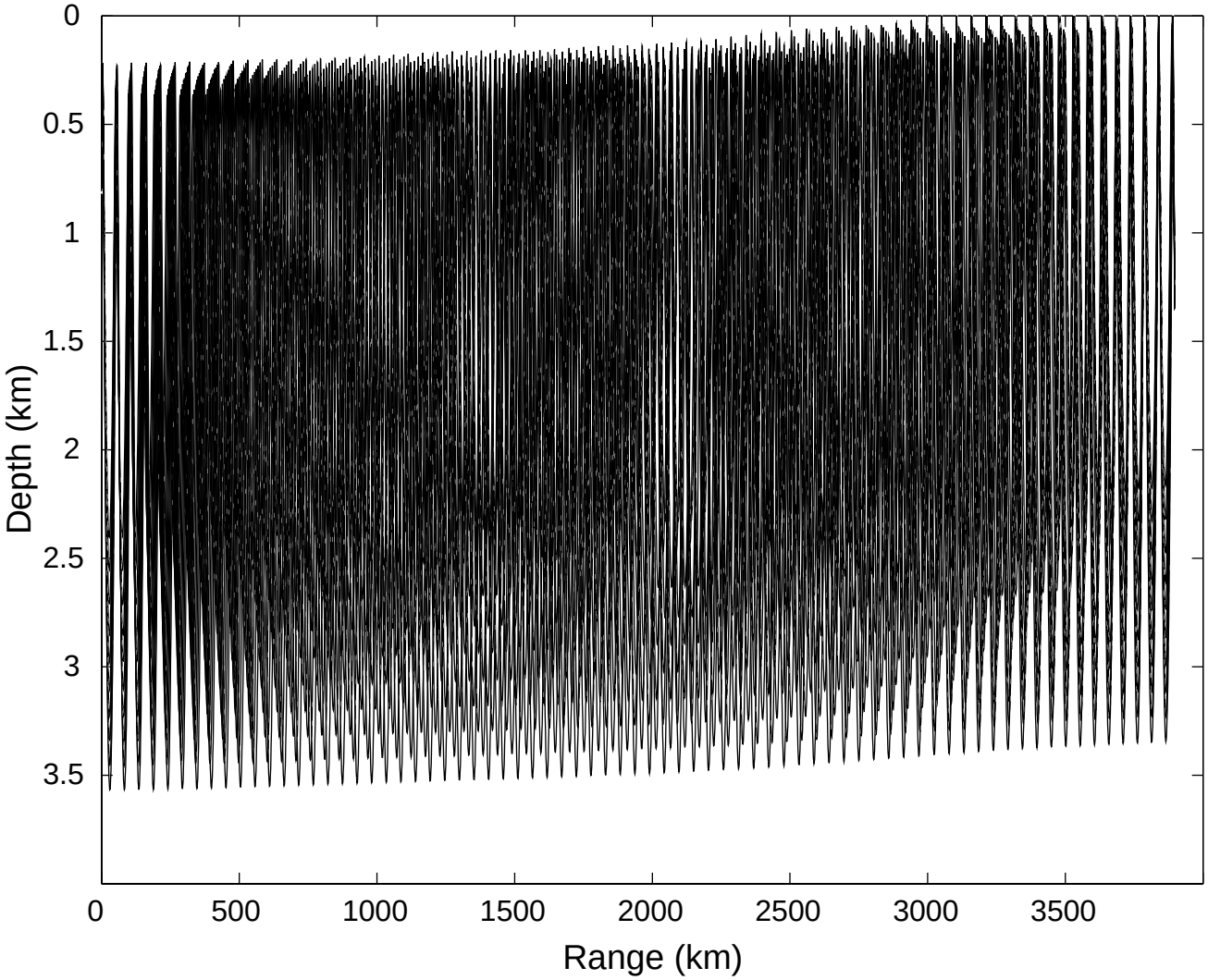

Figure 4. The ray paths associated with resolved ray arrivals for acoustic transmissions from Kauai to receiver **d**. Near Hawaii the ray paths do not sample the upper 100–200 m of the ocean, while near California the rays are surface reflecting, or near-surface refracting. These raypaths were derived using the annual mean Levitus ocean atlas.

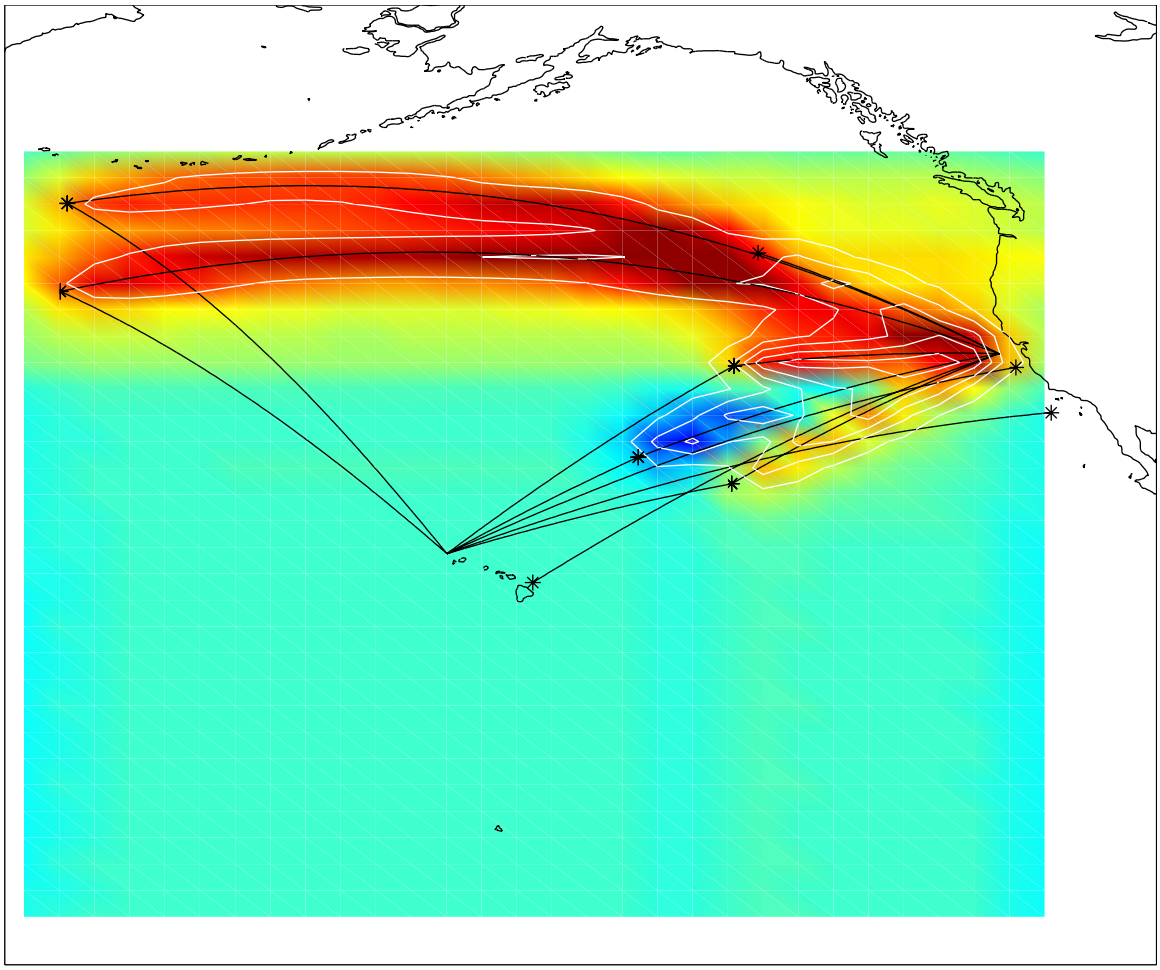

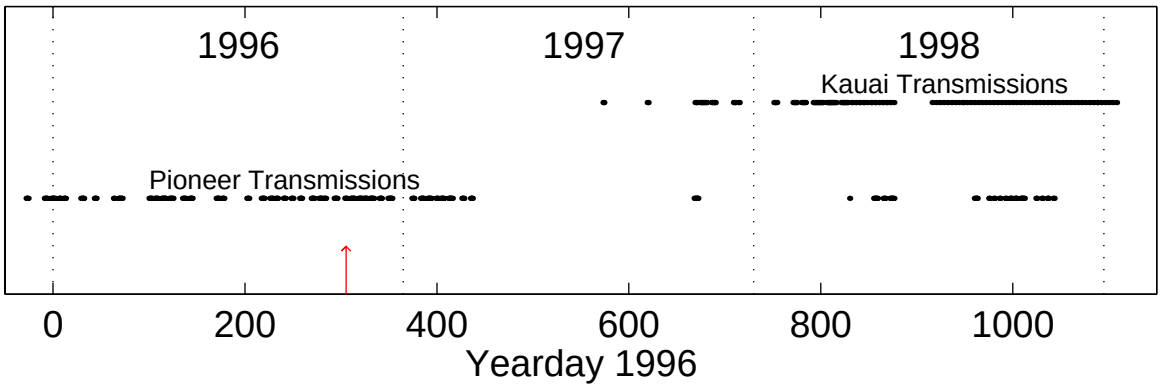
1996
1997
1998
Kauai Transmissions
Pioneer Transmissions
0
200
400
600
800
1000
Yearday 1996

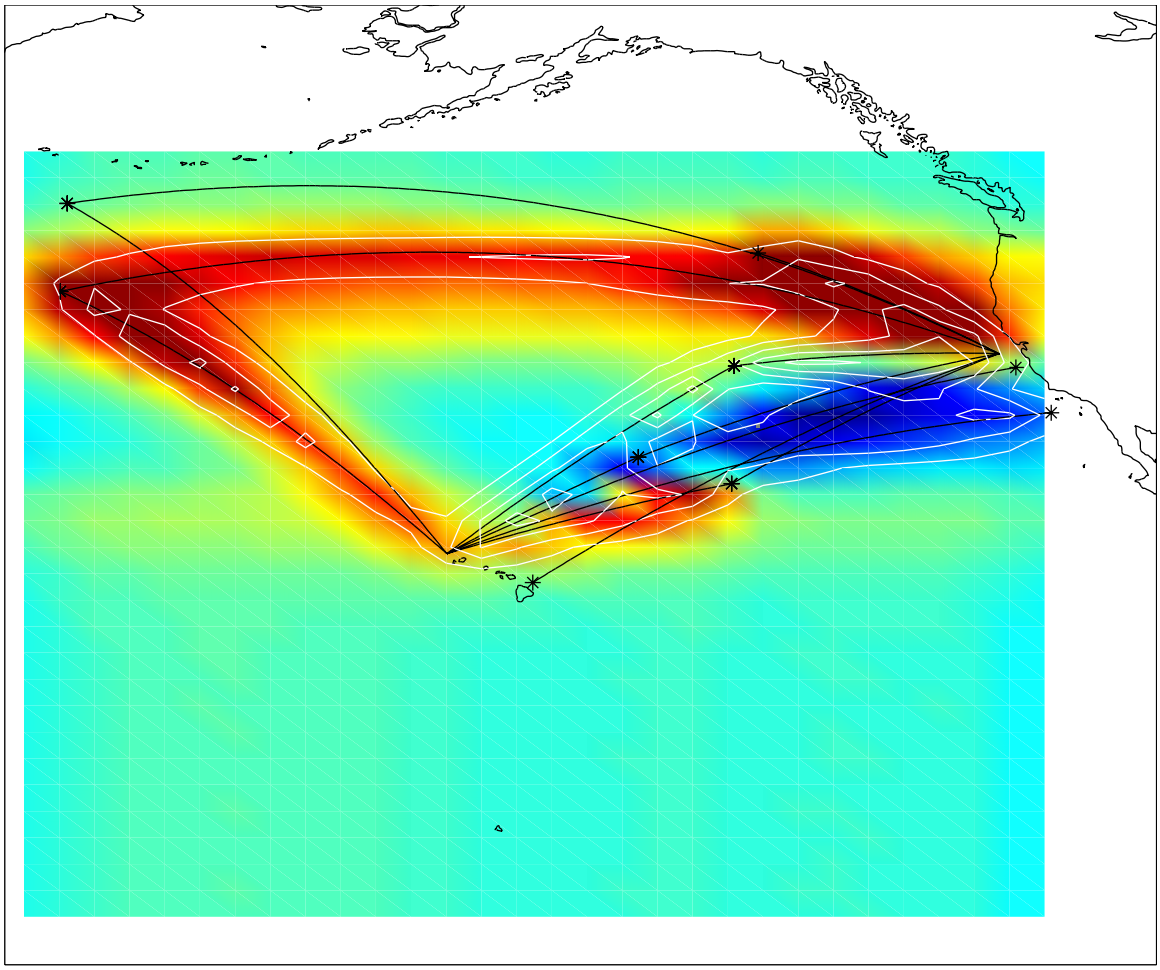

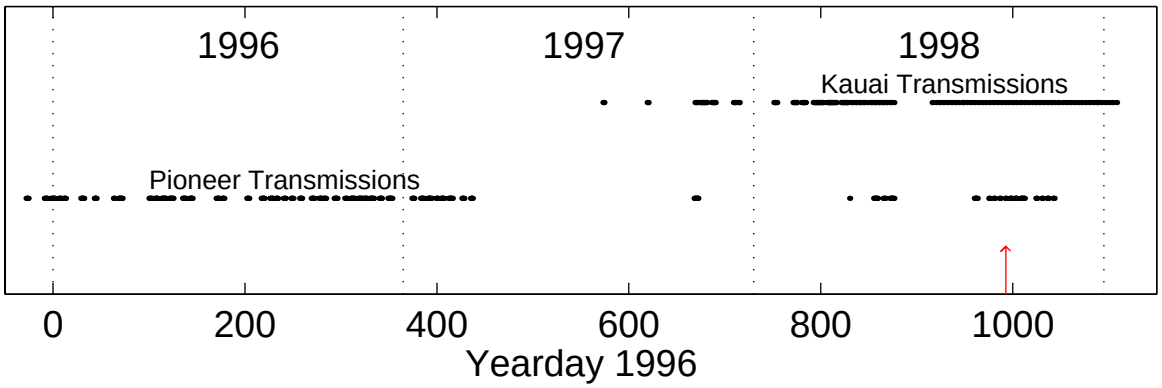
1996
1997
1998
Kauai Transmissions
Pioneer Transmissions
0
200
400
600
800
1000
Yearday 1996